

# Facile fabrication of highly flexible graphene paper for photocatalytic reduction of 4-nitrophenol

HUA CHEN<sup>1</sup>, GUOHUA JIANG<sup>1,2,3,\*</sup>, LEI LI<sup>1</sup>, YONGKUN LIU<sup>1</sup>, QIN HUANG<sup>1</sup>,  
TENG TENG JIANG<sup>1</sup> and XIANGXIANG DU<sup>1</sup>

<sup>1</sup>Department of Materials Engineering, Zhejiang Sci-Tech University, Hangzhou 310018, PR China

<sup>2</sup>National Engineering Laboratory for Textile Fiber Materials and Processing Technology (Zhejiang), Hangzhou 310018, PR China

<sup>3</sup>Key Laboratory of Advanced Textile Materials and Manufacturing Technology (ATMT), Ministry of Education, Hangzhou 310018, PR China

MS received 18 March 2015; accepted 20 May 2015

**Abstract.** Freestanding paper-like materials prepared from chemically derived graphene have considerable potential as a carbon-based catalyst in high-performance flexible catalytic reaction. Herein, a highly flexible graphene paper (GP) assembled from graphene oxides (GOs) with the aid of polyacrylamide (PAA) and electroless deposition of gold nanoparticles (AuNPs) was prepared. In contrast to previous reports on GOs based on a flow-directed assembly of graphene sheets, this GOs/PAA/Au composite paper exhibited a highly wrinkled and disordered morphology. The resultant GOs/PAA/Au composite paper was applied as a catalytic material for the reduction of 4-nitrophenol and showed the favour separation, recovery and cyclic utilization properties.

**Keywords.** Au; catalytic; composite; recycling.

## 1. Introduction

Graphene, as closely packed into two-dimensional (2D) nanomaterials, consisted of sp<sup>2</sup>-bonded carbon atoms and has potential applications in nanoelectronics, sensors, biodevices, batteries and drug delivery.<sup>1</sup> Moreover, graphene-based hybrids, as a kind of multifunctional assembly, have been received considerable attention in recent years.<sup>2</sup> Among them, the inclusion of electron-rich metal nanoparticles such as Au, Ag, Pt and Pd with graphene provides one of important routes to develop hybrid materials with potential applications in the field of surface enhanced Raman spectroscopy, field effect transistors, catalysis and biosensing.<sup>3</sup> These hybrid materials not only display the properties of metal nanoparticles and those of graphene, but also exhibit novel properties including lightweight, highly flexible and scalable features due to the interaction between metal nanoparticles and graphene.

In recent times, noble metallic nanoparticles have been found applications in many fields, such as optical biosensor,<sup>4</sup> electronic devices,<sup>5</sup> biomedical<sup>6</sup> and catalysis.<sup>7</sup> Especially, the gold nanoparticles (AuNPs) have received increasing attention due to their large surface area-to-volume ratio, and abundant active surface atoms display

outstanding catalytic activity and selectivity for many catalytic reactions, including hydrogenation,<sup>8</sup> oxidation<sup>9</sup> and C–C coupling reaction.<sup>10</sup> However, it is difficult to investigate the recoverable catalytic properties of these gold nano-catalytic systems because of their aggregation and tiny size for separation. To facilitate cyclic utilization of AuNPs catalysts, they are frequently attached on/in various solid supports, such as polymer,<sup>11</sup> metal oxide,<sup>12</sup> carbon materials<sup>13</sup> and natural materials,<sup>14</sup> fabricating hybrid nano-structural catalysts. Herein, a highly flexible graphene paper (GP) assembled from graphene oxides (GOs) with the aid of polyacrylamide (PAA) and electroless deposition of AuNPs was reported. In contrast to previous reports on GOs based on a flow-directed assembly of graphene sheets, this GOs/PAA/Au composite paper exhibited a highly wrinkled and disordered morphology. The resultant GOs/PAA/Au composite paper was applied as a catalytic material for the reduction of 4-nitrophenol (4-NP) and showed the favour separation, recovery and reuse properties.

## 2. Experimental

### 2.1 Preparation

In this research, the GOs solution was firstly fabricated on the basis of a modified Hummer's method.<sup>15</sup> Then, GOs (0.1 g l<sup>-1</sup>) and PAA (0.1 mol l<sup>-1</sup>) were mixed and

\*Author for correspondence (ghjiang\_cn@zstu.edu.cn)

stirred for about 2 h. The solutes in the resultant mixture were deposited on the filter membrane (pore size:  $\sim 0.1 \mu\text{m}$ ) with the assistance of a vacuum filtration system. After removal of solvent, the filter membrane was dried under temperature ranged from 60 to  $80^\circ\text{C}$ . During this process, the amino groups of PAA were reacted with oxygen-containing groups of GOs to form paper-like composite with multi-layer structure. Next, the dried GOs/PAA composite paper was immersed into chlorauric acid solution ( $0.1 \text{ mmol l}^{-1}$ ) under UV light irradiation. The AuNPs were immobilized on GOs with the dual reduction of UV light and amino groups. The schematic representation for the preparation of GOs/PAA/Au composite paper is shown in scheme 1.

## 2.2 Measurement of catalytic activity

The catalytic activity of the prepared flexible GP was evaluated by photometrically monitoring the reduction of 4-NP to 4-aminophenol (4-AP). Firstly, the prepared flexible GP ( $\sim 2 \times 4 \text{ cm}$ ) was added into 50 ml of 4-NP ( $C_{4\text{-NP}} = 1.73 \text{ mmol l}^{-1}$ ) solution. After introducing 2 ml of freshly prepared 0.17 M  $\text{NaBH}_4$  aqueous solution, the mixture was stirred under ambient conditions. The concentration of 4-NP in the solution was measured using a UV-vis spectrometer.

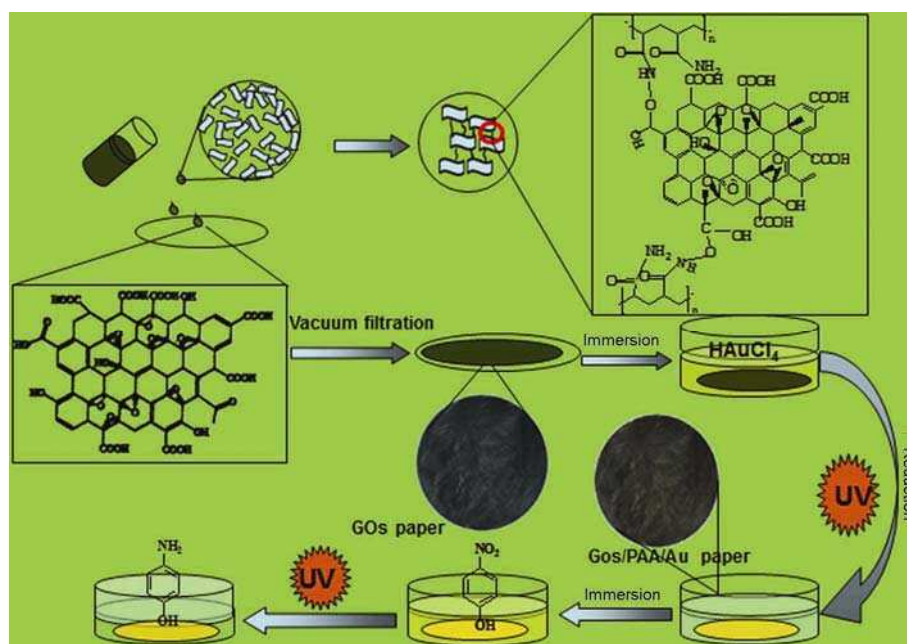
## 2.3 Characterization

The structures and crystal phase of the as-prepared samples were analysed with a SIEMENS Diffraktometer

D5000 X-ray diffractometer with  $\text{CuK}\alpha$  radiation source at 35 kV, with a scan rate of  $4^\circ \text{ s}^{-1}$  in the  $2\theta$  range of  $5\text{--}80^\circ$ . X-ray photoelectron spectroscopy (XPS) data were obtained with an ESCALab220i-XL electron spectrometer from VG Scientific using 300 W  $\text{AlK}\alpha$  radiation. The ULTRA-55 field emission scanning electron microscopy (FE-SEM) at an accelerating voltage of 10 kV and JSM-2100 transmission electron microscopy (TEM) was used to characterize the morphology of the as-prepared samples. Raman spectra were recorded using a microRaman spectroscopy (TriVista TR557 princeton Instruments). The concentration of 4-NP was measured by a JASCO V-570 UV-vis-NIR spectrophotometer (Japan). The Agilent high-performance liquid chromatography (HPLC) 1100 was used to confirm the products in the reaction.

## 3. Results and discussion

The photographs of paper-like GOs/PAA/Au composite with bright black colour are shown in figure 1a. It is interesting to note that the resultant GOs/PAA/Au composite paper is highly flexible. It can be bent over  $160^\circ$  for hundreds of cycles without any damage, as shown in figure 1a. FE-SEM and TEM are employed to determine the morphology and the size of AuNPs, respectively. Typical SEM and TEM images of the AuNPs deposited on GOs are shown in figure 1b and c, respectively. It can be found that AuNPs are uniformly dispersed on the GOs and the mean size of AuNPs is about 7.2 nm (inset in figure 1c). The crystalline nature of AuNPs deposited on GOs is further investigated by high-resolution TEM



**Scheme 1.** Schematic representation for the preparation of GOs/PAA/Au composite paper for photocatalytic reaction of 4-NP.

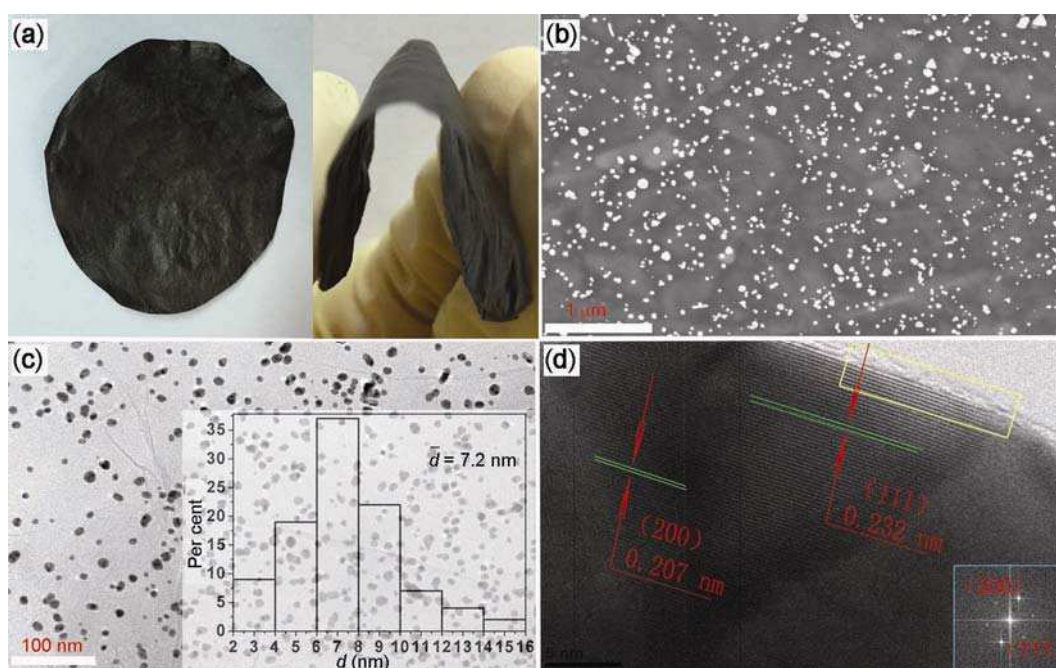


**Figure 1.** (a) Digital picture, (b) SEM image, (c) TEM image, inset shows the size distribution of AuNPs) and (d) HR-TEM image of GOs/PAA/Au composite paper, inset shows SAED pattern of AuNPs).

(HR-TEM). As shown in figure 1d, the lattice spacing of 0.207 and 0.232 nm can be assigned to the (200) and (111) planes of the Au crystal, respectively.<sup>16</sup> The inset of figure 1d is the selected area electron diffraction (SAED) image of AuNPs that indicates the single crystalline nature of AuNPs. At the edge of AuNPs, a layer membrane material can be observed (yellow block in figure 1d). It may be the PAA and GOs adsorbed on AuNPs.

Figure 2 shows the XRD patterns of the products prepared in this research. In the case of GOs' sample, it shows a sharp peak at 11.63°, corresponding to the (001) plane of GOs.<sup>17</sup> The characteristic peak still can be found in the GOs/PAA and GOs/PAA/Au composites. It indicates the structures of GOs do not change in the presence of PAA and Au. For the GOs/PAA/Au composite, two new distinctive peaks centred at ~38° and 44.5° can be observed. They are the typical signals of Au (111) and (200) lattice planes.<sup>18</sup> The average crystallite size from Scherrer's equation is 6.95 nm according to the Au diffraction pattern, which is close to the TEM results.<sup>19</sup>

The chemical composition of the obtained composites was further confirmed by XPS measurement. The XPS spectrum of the GOs/PAA/Au composite paper exhibit prominent peaks of N, O and relatively feeble peaks of Au, as shown in figure 3a. The high-resolution XPS spectrum of Au 4f on the GOs/PAA/Au composite paper is shown in figure 3b. Bond energies of 84.0 and 87.7 eV (AuNPs) correspond to pure Au.<sup>20</sup> Any deviation from these bond energies implies that the AuNPs are interacting with other elements.<sup>21</sup> In our case two bond

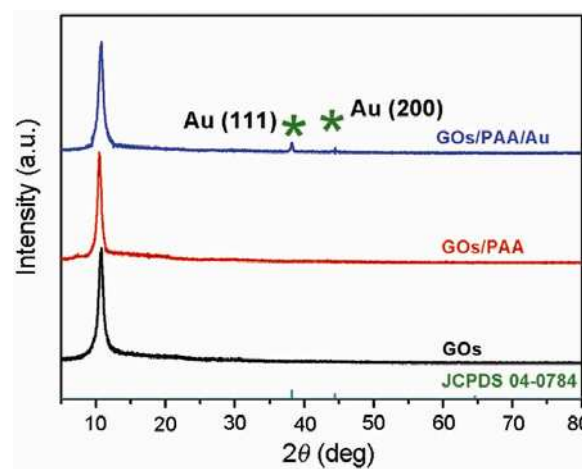


**Figure 2.** XRD patterns of the GOs paper, GOs/PAA paper and GOs/PAA/Au paper.

energies at 84.1 and 87.8 eV were obtained. This may suggest that the AuNPs have been formed with characteristic bond energy with substrate differing from the AuNPs alone. Figure 3c shows the carbon single/double bonds (C–C/C=C, peak 2, 284.8 eV), and oxygen-containing functional groups dominated by hydroxyl and epoxy groups (C–OH/C–O–C, peak 4, 286.6 eV) with relatively small amounts of carbonyl (C=O, peak 5, 287.8 eV) and carboxylic (COO, peak 1, 289.2 eV) groups.<sup>22</sup> The peak at 285.7 eV (peak 3) corresponds to the C–N from the PAA.<sup>23</sup> The high-resolution N spectrum displays a peak

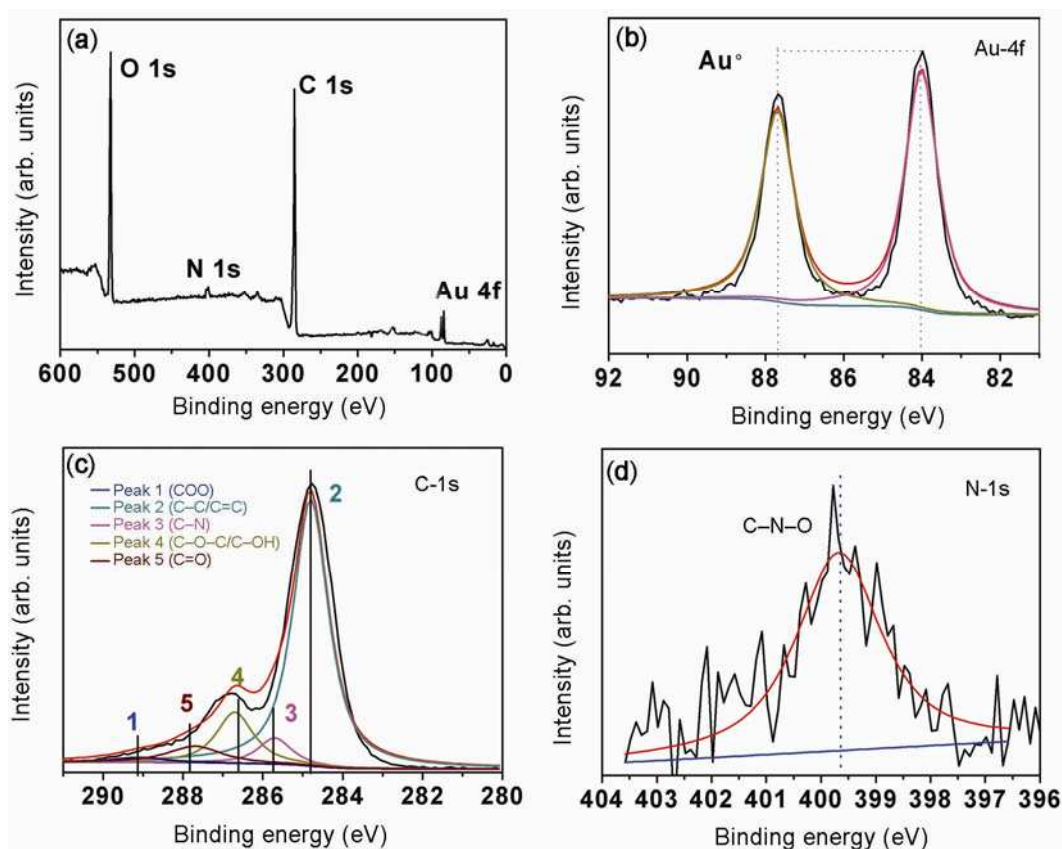


**Figure 3.** XPS spectra of (a) GOs/PAA/Au composite paper, (b) Au-4f XPS data, (c) C-1s XPS data and (d) N-1s XPS data.

at 399.6 eV, which is attributed to the C–N–O bond.<sup>24</sup> It implies the existence of interaction between PAA and GOs.

Raman spectroscopy is an excellent method to characterize and determine the microstructure of carbon nanomaterials. As shown in figure 4a, the Raman spectrum of GOs displays two prominent peaks at 1371 and 1587  $\text{cm}^{-1}$ , corresponding to the well-documented D and G bands, respectively. The D and G bands still can be found in GOs/PAA and GOs/PAA/Au products. However, the D/G intensity ratio is increased compared to that in GOs, as shown in figure 4b. The ratio of intensity of the D/G bands is a measure of the defects present on graphene structure. The G band is a result of in-plane vibrations of  $\text{sp}^2$  bonded carbon atoms, whereas the D band is due to out of plane vibrations attributed to the presence of structural defects.<sup>25</sup> The D/G intensity ratios for three products are 1.17, 1.21 and 1.23, respectively. It implies that the amount of GOs has been decreased due to the reduction of GOs in GOs/PAA and GOs/PAA/Au products.

The as-prepared GOs/PAA/Au products were tested as catalyst for the reduction of 4-NP under a 300 W lamp to provide UV light ( $\lambda \leq 400$  nm). In a typical experiment, the original absorption peak of 4-NP was centred at 317 nm in neutral or acidic conditions and shifted to 400 nm immediately upon the addition of  $\text{NaBH}_4$  due

to the formation of 4-nitrophenolate ions.<sup>26</sup> In the absence of our catalysts, the adsorption peak at 400 nm remained unaltered even for 1 week. However, when a proper amount of GOs/PAA/Au composite paper ( $\sim 2 \times 4$  cm) was present, the immediate decolourization of the 4-NP solution was clearly observed. After about 40 min, the peak at 400 nm almost completely disappeared, suggesting the end of the conversion (figure 5a). The products during the photocatalytic oxidation were determined by HPLC analysis. As shown in figure 5b, the relative retention times (RRT) of chromatographic peak of pure 4-AP and 4-NP are located at 1.7 and 4.2 min (inset figure 5b), respectively. After adding GOs/PAA/Au composite paper into the reactive system, the chromatographic peak of 4-NP peak is decreased and the one of 4-AP is increased as well. After irradiation for 30 min, two new chromatographic peaks located at 3 and 3.6 min can be observed, which are assigned to hydroxyl amino phenol and 4-nitrosophenol, respectively.<sup>27</sup> After reaction for 60 min, the chromatographic peak (4.2 min) of 4-NP disappeared and only the chromatographic peak at 1.7 min can be observed. It indicates 4-NP has been transformed to 4-AP.

The pseudo-first-order kinetics could be used to evaluate the kinetic reaction rate of the current catalytic

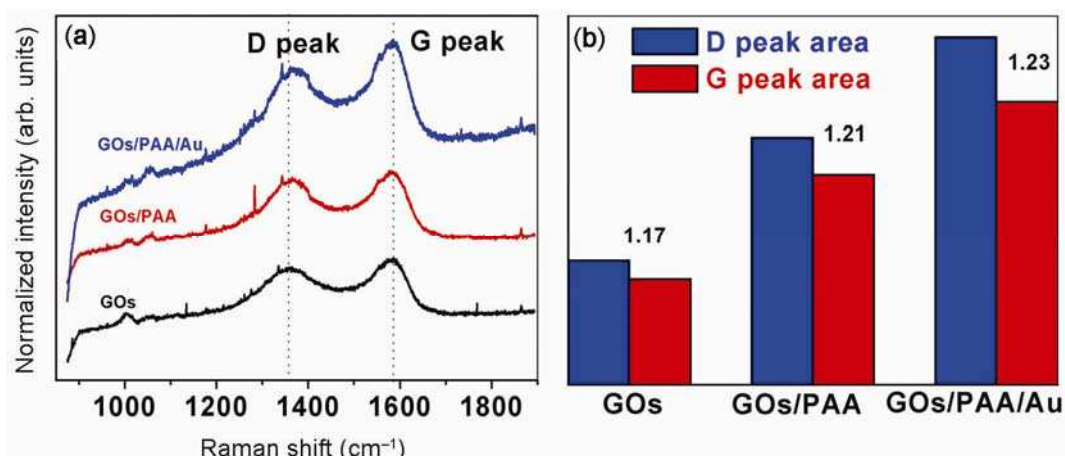


**Figure 4.** (a) Raman spectra of GOs, GOs/PAA and GOs/PAA/Au composite paper and (b) the D and G peak areas of GOs, GOs/PAA and GOs/PAA/Au composite paper.

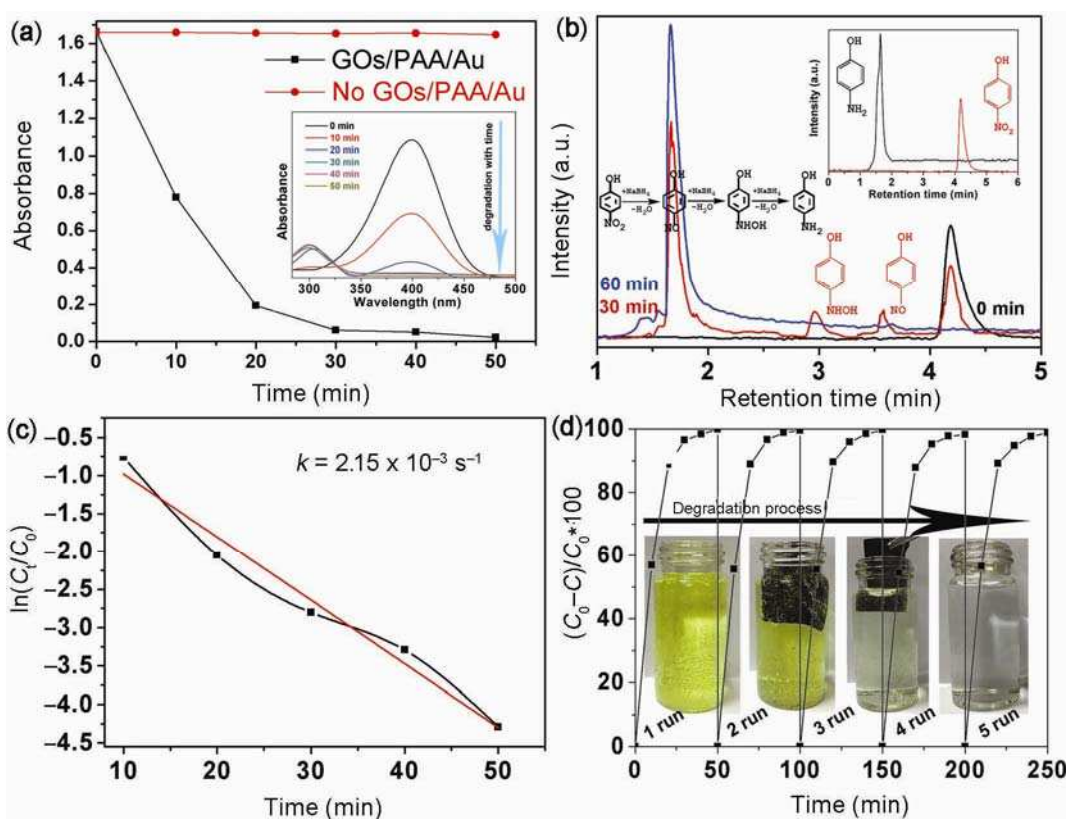
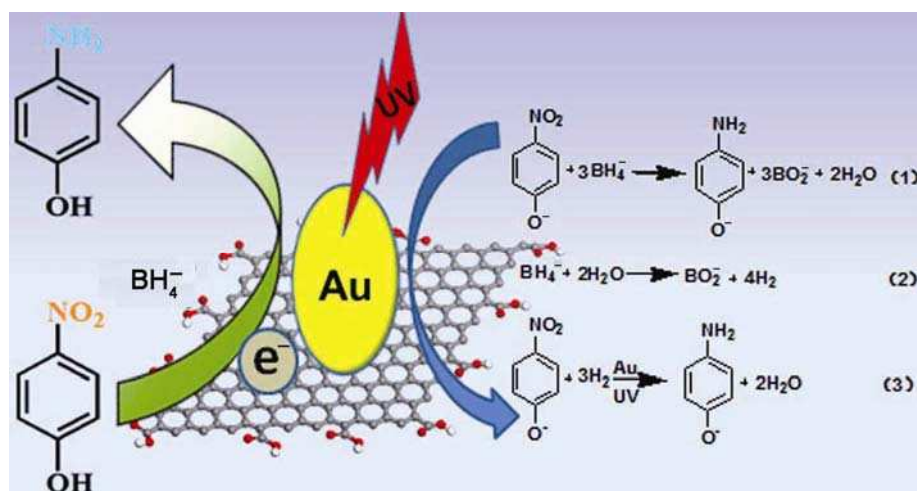


**Figure 5.** Time-dependent changes of the 4-NP solution with (a) presence of GOs/PAA/Au composite paper, (b) high-performance liquid chromatography curves, (c) the first-order reaction fitting curve and (d) the photos of degradation process and the recycle photocatalytic decolouration of 4-NP solution.

reaction. The kinetic rate constant  $k_{app}$  can be calculated from the rate equation  $\ln(C_t/C_0) = -k_{app}t$ , where  $C_0$  is the initial concentration of 4-NP and  $C_t$  represents the concentration of 4-NP at the time  $t$ . As shown in figure 5c, GOs/PAA/Au composite paper exhibits a high activity with an estimated  $k_{app}$  value of  $2.15 \times 10^{-3} \text{ s}^{-1}$ , which is

better than AuNPs'  $k_{app}$  value of  $2.1 \times 10^{-3} \text{ s}^{-1}$ .<sup>28</sup> Figure 5d shows the photographs of the degradation process. To illustrate the superiority of our support, the recycle experiment on the catalytic reduction of 4-NP is carried out. The efficiency of catalytic reduction is still maintained without significant decline even after five cycles,



**Scheme 2.** Mechanism for reduction of 4-nitrophenol over the GOs/PAA/Au composite paper.

indicating the excellent durability of GOs/PAA/Au composite paper.

The possible mechanism of 4-NP degradation is shown in scheme 2. GOs with large surface area and extraordinary electronic transport properties are beneficial to transport electrons. Meanwhile, GOs also can be utilized as a support to disperse and stabilize AuNPs due to their strong mechanical strength.<sup>29</sup> 4-NP can be adsorbed onto GO via  $\pi$ - $\pi$  stacking interactions for its  $\pi$ -rich nature. It provides a high concentration of 4-NP near to the AuNPs, leading to a high efficient contact between them.<sup>30</sup> Under UV light irradiation, the AuNPs relay electrons from the donor  $\text{BH}_4^-$  to the acceptor 4-NP.<sup>31</sup> The transformation of 4-NP to 4-AP can be expressed by equations (1–3). Equation (1) is the total reaction. The  $\text{BH}_4^-$  reacts with  $\text{H}_2\text{O}$  to produce hydrogen radicals. And with the addition of protons to the 4-NP and the simultaneous removal of its oxygen, the 4-NP is reduced by  $\text{H}_2$  transforming into 4-AP, as shown in equations (2) and (3).<sup>32</sup>

#### 4. Conclusion

In this work, the GOs/PAA/Au composite paper is prepared easily via a facile and environmental-friendly route. The resultant composite paper exhibited efficient catalytic activity for the reduction of 4-NP. Moreover, the catalyst can be easily separated from liquid environment due to its large size. The composite paper offers significant advantages, such as low dosage, high catalytic activity, easy recycling and excellent stability.

#### Acknowledgements

This work was financially supported by the National Natural Science Foundation of China (51373155, 51133006)

and ‘521 Talents Training Plan’ in Zhejiang Sci-Tech University (ZSTU).

#### References

- Raj M A and John S A 2015 *RSC Adv.* **5** 4964; Kim M, Kim D Y and Kang Y 2015 *RSC Adv.* **5** 3299
- Fang Y, Jiang G H, Wang R J, Wang Y, Sun X K, Wang S and Wang T 2012 *Bull. Mater. Sci.* **35** 495; Xu Q H, Gong Y W, Fang Y, Jiang G H, Wang Y, Sun X K and Wang R J 2012 *Bull. Mater. Sci.* **35** 795; Zhou Y, Xu F M, Jiang G H, Wang X H, Wang R J, Hu R B, Xi X G, Wang S, Wang T and Chen W X 2012 *Powder Technol.* **230** 247
- Kuru C, Choi D, Choi C, Kim Y J and Jin S 2015 *J. Nanosci. Nanotechnol.* **15** 2464; Xu G W, Lu R, Liu J, Hui R and Wu J Z 2014 *Adv. Opt. Mater.* **2** 729; You J M, Kim D, Kim S K, Kim M S, Han H S and Jeon S 2013 *Sens. Actuators B: Chem.* **178** 450
- El-Sayed I, Huang X H, Macheret F, Humstoe J O, Kramer R and El-Sayed M 2007 *Technol. Cancer Res. Treat.* **6** 403
- Didiot C, Pons S, Kierren B, Fagot-Revurat Y and Malterre D 2007 *Nat. Nanotechnol.* **2** 617
- Zhao J, Jensen L, Sung J, Zou S G, Schatz G C and Richard P 2007 *J. Am. Chem. Soc.* **129** 7647
- Ji Z Y, Shen X P, Xu Y L, Zhu G X and Chen K M 2014 *J. Colloid Interface Sci.* **432** 57
- Imada Y, Osaki M, Noguchi M, Maeda T, Fujiki M, Kawamorita S, Komiya N and Naota T 2015 *ChemCatChem* **7** 99
- Ferentz M, Landau M V, Vidruk R and Herskowitz M 2015 *Catal. Today* **241** 63
- Rej S, Chanda K, Chiu C Y and Huang M H 2014 *Chem. Eur. J.* **20** 15991
- Zhang W, Liu B, Zhang, Bian G, Qi Y, Yang X and Li C 2015 *Colloid Surf. A* **466** 210; Wang S, Zhang J, Yuan P, Sun Q, Jia Y, Yan W, Chen Z and Xu Q 2015 *J. Mater. Sci.* **50** 1323

12. Frydendal R, Busch M, Halck N B, Paoli E A, Krttil P, Chorkendorff I and Rossmeisl J 2015 *ChemCatChem* **7** 149
13. Lee J, Ahmed S R, Kim J, Suzuki T, Parmar K, Park S S, Lee J and Park E Y 2015 *Biosens. Bioelectron.* **64** 311
14. Nowinski A K, White A D, Keefe A J and Jiang S 2014 *Langmuir* **30** 1864
15. Hummers W S and Offeman R E 1958 *J. Am. Chem. Soc.* **80** 1339;  
Park S and Ruoff R S 2009 *Nat. Nanotechnol.* **4** 217
16. Li C, Cai W, Cao B, Sun F, Li Y, Kan and Zhang L 2006 *Adv. Funct. Mater.* **16** 83
17. Raghavan N, Thangavel S and Venugopal G 2015 *Mater. Sci. Semiconduct. Process.* **30** 321
18. Bott-Neto J L, Garcia A C, Oliveira V L and Tremiliosi-Filho G 2014 *J. Electroanal. Chem.* **735** 57
19. MSarma T K, Chowdhury D, Paula A and Chattopadhyay A 2002 *Chem. Commun.* **10** 1048
20. Sylvestre J, Poulin S, Kabashin A V, Sacher E, Meunier M and Luong J 2004 *J. Phys. Chem. B* **108** 16864
21. Maringa A, Mashazi P and Nyokong T 2015 *J. Colloid Interface Sci.* **440** 151
22. Kim D, Yang S J, Kim Y S, Jung H and Park C R 2012 *Carbon* **50** 3229
23. Allen G C, Hallam K R, Eastman J R, Graveling G J, Ragnarsdottir V K and Skuse D R 1998 *Surf. Interface Anal.* **26** 518
24. Yang S J, Kang J H, Jung H, Kim T and Park C R 2013 *J. Mater. Chem. A* **1** 9427
25. Stankovich S, Dikin D A, Piner R D, Kohlhaas K A, Kleinhammes A, Jia Y, Wu Y, Nguyen S T and Ruoff R S 2007 *Carbon* **45** 1558
26. Tian J, Liu G, Guana C and Zhao H 2013 *Polym. Chem.* **4** 1913
27. Brezov V, Blakovi B, Surina I and Havlfnova B 1997 *J. Photochem. Photobiol. A – Chem.* **107** 233
28. Rashid H, Bhattacharjee R R, Kotal A and Mandal T K 2006 *Langmuir* **22** 7141
29. Vix-Guterl C, Frackowiak E, Jurewicz K, Friebe M, Parmentier J and Béguin F 2005 *Carbon* **43** 1293
30. Lu W, Ning R, Qin X, Zhang Y, Chang G, Liu S, Luo Y and Sun X 2011 *J. Hazard. Mater.* **197** 320
31. Harish S, Mathiyarasu J and Phani K 2009 *Catal. Lett.* **128** 197
32. Huang J, Vongehr S, Tang S, Lu H and Meng X 2010 *J. Phys. Chem. C* **114** 15005